An Application of Compressive Sensing for Image Fusion

Tao Wan
Department of Electrical and Electronic Engineering
University of Bristol
Bristol, BS8 1UB, UK

Zengchang Qin*
Intelligent Computing and Machine Learning Lab
School of Automation Science and Electrical Engineering
Beihang University, Beijing, 100191, China

ABSTRACT

Compressive sensing(CS) has inspired significant interest because of its compressive capability and lack of complexity on the sensor side. In this paper, we present a study of three sampling patterns and investigate their performance on CS reconstruction. We then propose a new image fusion algorithm in the compressive domain by using an improved sampling pattern. There are few studies regarding the applicability of CS to image fusion. The main purpose of this work is to explore the properties of compressive measurements through different sampling patterns and their potential use in image fusion. The study demonstrates that CS-based image fusion has a number of perceived advantages in comparison with image fusion in the multiresolution (MR) domain. The simulations show that the proposed CS-based image fusion algorithm provides promising results.

Categories and Subject Descriptors

I.4.8 [**Image Processing and Computer Vision**]: Scene Analysis—*sensor fusion*; G.1.6 [**Numerical Analysis**]: Optimization—*linear programming*

General Terms

Algorithms,Experimentation,Performance

Keywords

compressive sensing, CS-based image fusion, multiresolution image fusion

1. INTRODUCTION AND MOTIVATION

*Corresponding author.
E-mail address: zcqin@buaa.edu.cn

CIVR '10, July 5-7, Xi'an China

Results of Candès *et al.* [6] and Donoho [9] demonstrated that sparse or compressible signals can be accurately reconstructed from a small set of incoherent projections, in what is now known as compressive sensing or compressive sampling. Usually, the number of samples required for reconstructing the original signal can be far fewer than the number of samples if the signal is sampled at the Nyquist rate, thus providing the benefits of reduced storage space and transmission bandwidth due to the phenomenal compression achieved. For this reason CS has been proposed as a viable candidate in many practical applications, such as data compression [3, 7], wireless communication [18], sensor networks [4], compressive imaging [8, 10], etc. However, there is little literature on CS concerning its application to image fusion. Image fusion is the combination of multiple images into a single fused image that aids human visual perception or subsequent image processing tasks. One method of achieving image fusion is with a multiresolution decomposition scheme [15, 25]. All these methods require knowledge of the original images. A natural question emerges about the possibility of fusing images without acquiring the original input images. One key advantage offered by the CS approach is that samples can be collected without assuming any prior information about the signal being observed, thereby motivating our research on compressive image fusion.

In this paper, we first analyze the impact of different sampling patterns on the compressive sensing reconstruction. For this purpose, three patterns are employed to sample the image in the Fourier domain similar to [5]. The image is then recovered via a total variation optimization presented in [6]. The performance of the sampling patterns is tested on various types of images, especially, on multimodal images, which are used in the proposed CS-based image fusion algorithm. Finally, an image fusion algorithm is presented in the compressive domain using different sampling patterns. The experiments show that our proposed double-star-shaped pattern achieves better reconstruction results as well as fusion results. Due to its universality and simplicity on the hardware side [10], compressive sensing is an attractive scheme for image fusion. CS-based image fusion possesses a number of advantages over conventional image fusion in the multiresolution domain. These are discussed in Section 4.

The remainder of the paper is organized as follows. Section 2 provides a brief description on CS and introduces new

sampling patterns with their performance on the compressive sensing reconstruction. In Section 3, a new CS-based image fusion algorithm is developed in comparison with a conventional image fusion technique in the multiresolution domain. Simulation results and discussions are presented in Section 4. Finally, conclusions and suggestions for future work are given in Section 5.

2. SAMPLING PATTERNS IN COMPRESSIVE SENSING

Compressive sensing enables a sparse or compressible signal to be reconstructed from a small number of non-adaptive linear projections, thus significantly reducing the sampling and computation costs. CS has many promising applications in signal acquisition, compression and medical imaging [17, 19]. In this work, we investigate its potential application in the image fusion. We first provide a brief introduction to compressive sensing and explore the impact of different sampling patterns on the CS reconstruction.

2.1 Background on Compressive Sensing

Consider a real-valued, finite-length, one-dimensional signal[1] $\mathbf{x} \in \mathbb{R}^N$ with elements $x[n], n = 1, 2, ..., N$. We say that the signal is K-sparse if it can be represented as:

$$\mathbf{x} = \Psi\boldsymbol{\theta} \tag{1}$$

where Ψ is some basis and $\boldsymbol{\theta}$ is a vector containing only $K \ll N$ nonzero coefficients. $\boldsymbol{\theta}$ can be thought of as $\mathbf{x}$ in domain Ψ. In CS, we do not measure or encode $\boldsymbol{\theta}$ directly, rather, we take the compressive measurements:

$$\mathbf{y} = \Phi\mathbf{x} \tag{2}$$

where $\mathbf{y} \in \mathbb{R}^M$ and Φ is an $M \times N$ matrix representing the measurement process. Although $M < N$ makes the recovery of the signal $\mathbf{x}$ from the measurements $\mathbf{y}$ ill-posed in general, recent CS experiments show that the recovery is possible and practical by adding assumption of signal sparsity [20].

2.2 Sampling Patterns in CS Measurement

From Section 2.1, it is known that compressive measurements $\mathbf{y}$ are obtained from a non-adaptive linear projection of the signal onto a random measurement basis matrix Φ. There are different ensembles of CS matrices defined in previous CS literature. For example, in [9], Donoho considered a uniform spherical ensemble, and Candès *et al.* used random partial Fourier matrices and showed several interesting properties of this ensemble in CS [6]. Due to the special structure of the Fourier transform underlying the partial Fourier ensemble, the use of such matrices greatly expands the applicability of the CS scheme into large scale data, e.g. 2-D images [20]. For example, a toolbox called *l*1-magic [5] used 2-D fast Fourier transform and the CS matrix Φ was constructed by a star-shaped sampling pattern in the 2-D Fourier plane, as shown in Fig. 1(a). The sampling pattern consists of white lines indicating the locations of the frequencies used to compute compressive measurements $\mathbf{y}$.

[1]An image can be vectorised into a long one-dimensional vector.

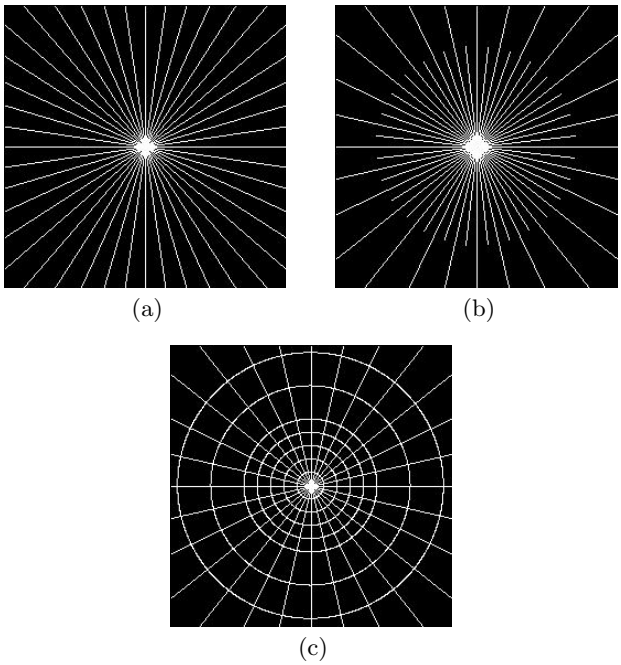

Figure 1: Sampling patterns. (a) Star shape. (b) Double-star shape. (c) Star-circle shape.

Once $\mathbf{y}$ have been measured, a reconstruction algorithm is employed to recover original signal $\mathbf{x}$ from the measurements $\mathbf{y}$. Therefore, the choice of different sampling patterns will lead to different measurements. There are two issues which need to be addressed: how the sampling patterns affect the reconstruction process, and whether a sampling pattern with superior performance to the star-shaped one can be found.

To investigate these problems, we design two new sampling patterns according to the properties of the 2-D Fourier transform by ensuring that the number of compressive samples remains the same as for the star-shaped one. As we know, the low frequencies are centered at the origin of the frequency coordinate system and the high frequencies are away from the center. Images usually have lots of low frequency information, so the lines are chosen with higher density sampling at low frequency, like two stars centered at the same origin. We name the pattern "double-star", shown in Fig. 1(b). Inspired by the Gabor filter which divides the spectrum into slices, we design a pattern with a similar structure which also has higher density sampling at low frequency. The pattern is called "star-circle" shown in Fig. 1(c). By changing the density of lines in the sampling patterns, we can obtain different numbers of measurements.

All three patterns illustrated in Fig. 1 are tested on various types of images, including 40 natural images [2], 35 infrared (IR) and 35 visible images captured by the digital cameras. [1]. These surveillance images are also used in the following image fusion experiments. Fig. 2 presents the peak signal- to-noise ratio of the recovered images for these three sampling patterns. The M/N on the x-axis is the rate of the CS measurements over the original signal. The figure shows that better quality images can be obtained by simply taking

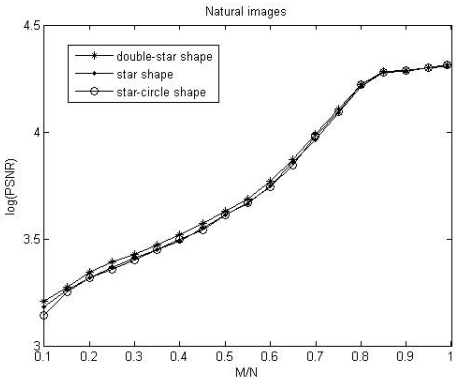

(a)

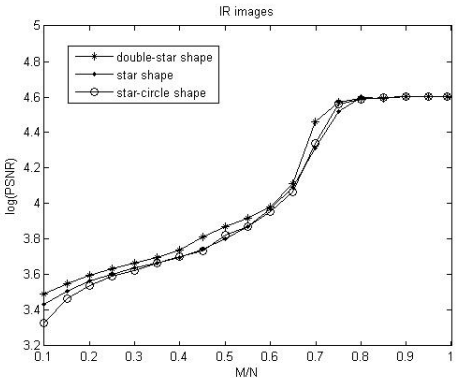

(b)

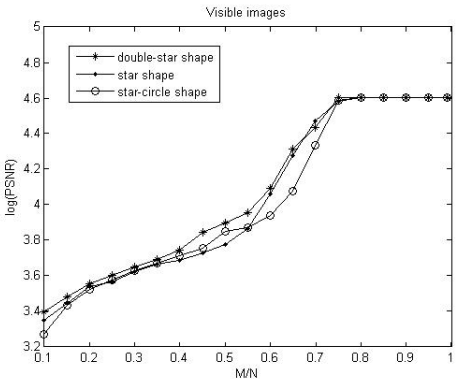

(c)

Figure 2: Log values of PSNR for reconstructions of a variety of images. (a) Natural images. (b) IR images. (c) Visible images.

more measurements because the CS measurement process is progressive. In these three cases, the double-star-shaped pattern yields the best performance for all the three types of images in terms of the PSNR values. We also notice that the reconstruction process demands less computation time by using the double-star-shaped pattern. This is because this sampling pattern makes a good balance of choosing the low frequencies and high frequencies in the Fourier domain.

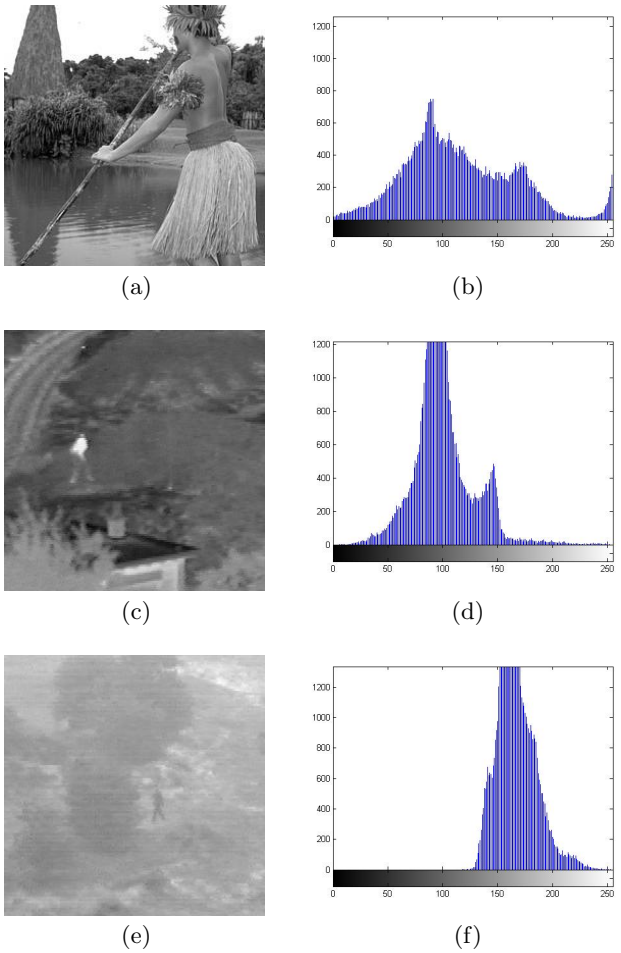

(a) (b) (c) (d) (e) (f)

Figure 3: Histograms of grayscale distributions for three images. (a) A natural image. (b) Histogram for the natural image (the standard deviation is $\sigma = 62.66$). (c) An IR image. (d) Histogram for the IR image (the standard deviation is $\sigma = 26.57$). (e) A visible image. (f) Histogram for the visible image (the standard deviation is $\sigma = 17.85$). The grayscale values are measured on a $0 - 255$ scale.

Moreover, visible and IR images' curves appear to be flat as a high proportion of the measurements are used for the reconstruction. This is because that the PSNR value is not available when the reconstruction algorithm generates a perfectly restored image that is identical to the original input image. In this case, we assume that the reconstructed image has 100 dB of PSNR (i.e. $log(100) = 4.61$) since the image estimated can hardly be distinguished from the original at a PSNR of about 60 dB [11]. However, the average experimental results show that natural images do not lead to a perfect reconstruction even by entailing more measurements. Additionally, there is a notable difference between natural images and visual and IR images in that the latter two types of images achieve a better PSNR with the same or fewer CS measurements. This can be explained using Fig. 3 which is an example showing the typical plotted histograms corresponding to these three types of images. The

standard deviation is used here to measure the dispersion of the grayscale image data. The real signals of the natural image tend to be less sparse than the visible and IR images. We know that signal sparsity is one of the important assumptions adopted in the CS reconstruction. Thus, natural images require more CS measurements to achieve a desirable threshold of PSNR (i.e. 60 dB or $log(60) = 4.09$) or fail to reach this value for some particular images. It is sensible to apply compressive sensing techniques to multisensor images.

3. COMPRESSIVE IMAGE FUSION

There is, to our knowledge, little research regarding the applicability of CS to image fusion in literature. The center piece of this work is to develop a new image fusion algorithm making good use of compressive sensing technique. We start with classic image fusion methods using multiresolution decompositions.

3.1 Image Fusion in the Multiresolution Domain

Multiresolution decompositions (e.g. pyramid, wavelet, linear, etc.) have shown significant advantages in the representation of signals. They capture the signal in a hierarchical manner where each level corresponds to a reduced-resolution approximation. MR methods in image fusion are very important for various reasons. First, MR representations enable one to consider and fuse image features separately at different scales. They also produce large coefficients near edges, thus revealing salient information [13]. Moreover, MR methods offer computational advantages and appear to be robust. In past decades, wavelets have emerged as an effective tool for this problem due to their energy compaction property [15, 22, 24]. In this paper, we address the image fusion problem in the context of wavelet transforms. As our main focus is not on MR image fusion, we choose a simple maximum selection (MS) fusion scheme to fuse the input images at the pixel level. MS is a widely used fusion rule which considers the maximum absolute values of the wavelet coefficients from the source images as the fused coefficients.

The wavelet-based image fusion algorithm consists of two main components. First, the detailed wavelet coefficients are composed using the MS fusion rule:

$$D_F = D_M \quad with \quad M = arg \max_{i=1,\ldots,I}(|D_i|) \tag{3}$$

where D_F are the composite coefficients, D_M is the maximum absolute value of the input wavelet coefficients, and I is the total number of the source images.

Because of their different physical meaning, the approximation and detail images are usually treated by the combination algorithm in different ways. Then a popular way to construct the fused approximation image A_F is:

$$A_F = \frac{1}{I}\sum_{i=1}^{I}(A_i) \tag{4}$$

The fused image is obtained by taking an inverse wavelet transform. As we can see, an image fusion approach based on wavelets requires to manipulate detailed coefficients and approximation images, while in the compressive domain, it only considers the compressive measurements.

Table 1: Compressive image fusion algorithm.

Algorithm: Compressive image fusion
1. Take the compressive measurements $Y_i, i = 1, ..., I$ for the i^{th} input image using the double-star-shaped sampling pattern.
2. Calculate the fused measurements using the formula: $Y_F = Y_M \quad with \quad M = arg\max_{i=1,\ldots,I}(\lvert Y_i\rvert)$.
3. Reconstruct the fused image from the composite measurements Y_F via the total variation optimization method [6].

3.2 Image Fusion in the Compressive Domain

In this section, we formulate an image fusion algorithm that uses compressive measurements to fuse multiple images into a single representation. Recent theoretical results show if the signal is sparse or nearly sparse in some basis, then with high probability, the measurements essentially encode the salient information in the signal. Further, the unknown signal can be estimated from these compressive measurements to within a controllable mean-squared error [6, 9]. In this sense, we can apply a similar fusion schemes to that used in the wavelet domain in the compressive domain, so the difference is that image fusion is performed on the compressive measurements rather than on the wavelet coefficients. The basic steps are described in Table 1.

There is a significant number of CS literature focusing on problems in signal reconstruction and image approximation. For instance, one technique employs a specialized interior-point method for solving CS reconstruction in which a preconditioned conjugate gradient method is used to compute the search step [12]. These methods generally rely on nonlinear recovery algorithms based on convex optimization and signals can be recovered from what appears to be highly incomplete data. Among them, $l1$-magic [5] based on the methodology proposed in [6] achieves robust and reliable reconstructed results, particularly for signals that are not strictly sparse. Our CS-based fusion algorithm adopts this reconstruction method to restore the resultant fused images. One drawback of this method is the high computational cost.

4. SIMULATION RESULTS AND DISCUSSIONS

Objective evaluation criteria are applied to compare fusion results obtained using different sampling patterns. Since ground-truth data are not available here, Piella's [16] and Petrovic's [14] metrics are used to measure the relative amount of salient information conveyed in the fused image. Three pairs of images shown in Fig. 4 are used in the experiments. In Fig. 5 and Fig. 6, we present some results of the proposed image fusion algorithm applied to these text images using Piella's and Petrovic's metrics, respectively. There is a clear performance improvement by using the double-star-shaped sampling pattern over the other two patterns when fewer measurements are used. However, all three patterns yield similar results as numbers of the compressive measure-

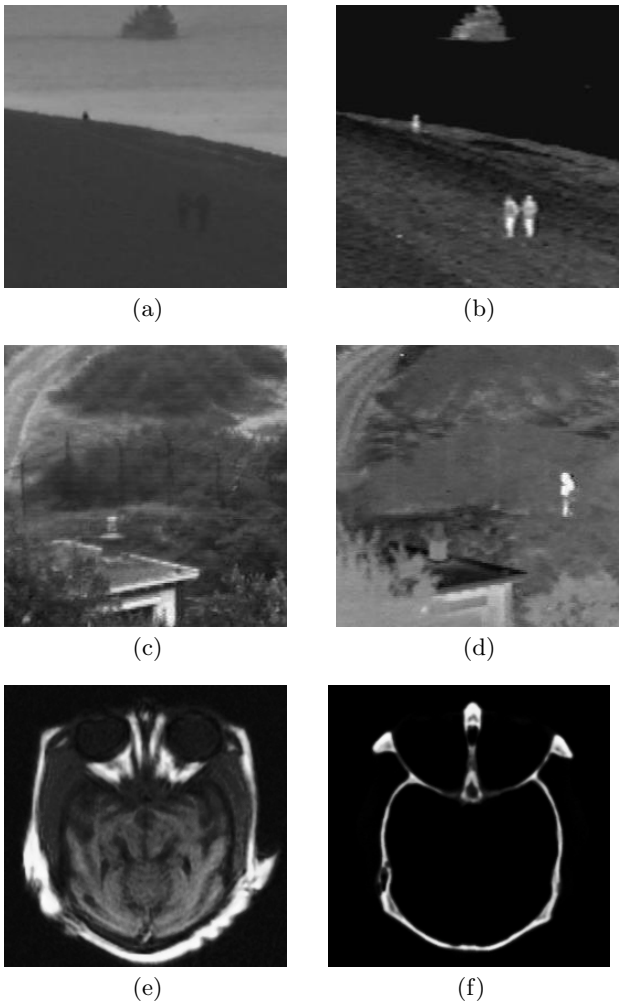

Figure 4: Experimental images. (a) 256×256 **"Kayak" visible image. (b)** 256×256 **"Kayak" IR image. (c)** 256×256 **"UN Camp" visible image. (d)** 256×256 **"UN Camp" IR image. (e)** 256×256 **MRI image. (f)** 256×256 **CT image.**

ments increase. The shape of the plotted polylines demonstrates that the two metrics generally offer correlated fusion assessment results. We notice that by using nearly 50% fewer compressive measurements than reconstructed pixels, we can achieve almost the same fusion results as using the entire set of pixels. Fig. 7(a)-(e) illustrate the fusion results using 10%, 25%, 50%, 75%, and all Fourier coefficients as the compressive measurements. The original input images are presented in Fig. 4(a) and 4(b). It indicates that there is no perceivable difference between the fused images using the measurements over 50% of Fourier coefficients.

Furthermore, compared with the fused image shown in Fig. 7(f) that is obtained by using a MS scheme in a complex wavelet domain, our proposed fusion algorithm does not provide a comparable results in terms of human perception. The poor image quality is mainly due to the fact that Fourier coefficients have their own limitations as compressive measurements to be used in image fusion. This has

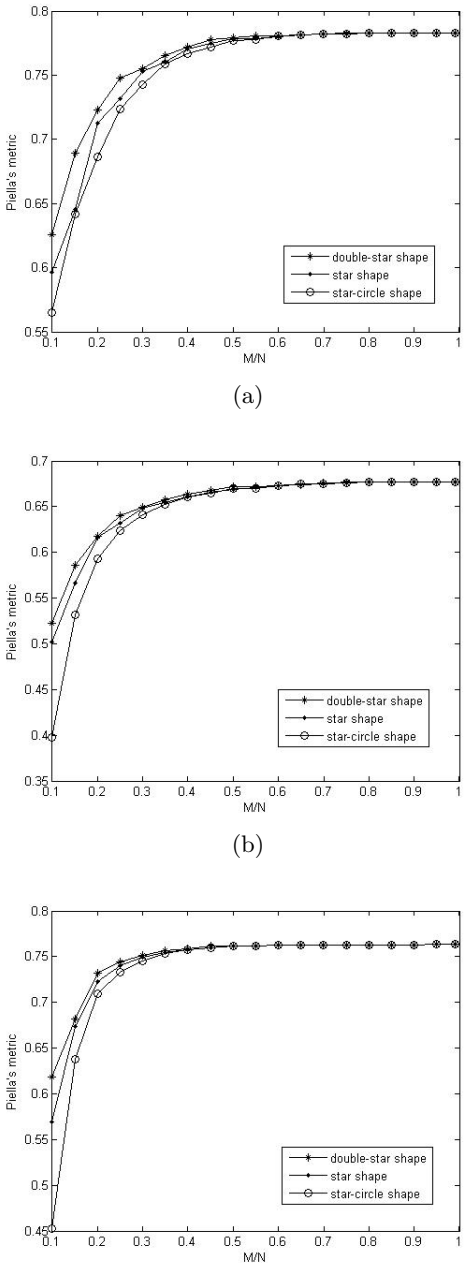

Figure 5: Piella's metric results using different sampling patterns for different images. (a) "Kayak" images. (b) "UN Camp" images. (c) Medical images.

been proven by observing Fig. 7(e). The reconstruction algorithm should also be accounted for in this case since the method was originally applied to one single image rather than multiple images.

Although the obtained fusion results are not perfect, CS-based image fusion has a number of advantages over conventional image fusion algorithms. It offers computational and storage savings by using a compressive sensing technique.

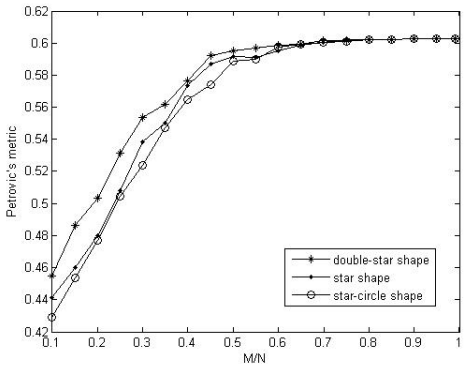

(a)

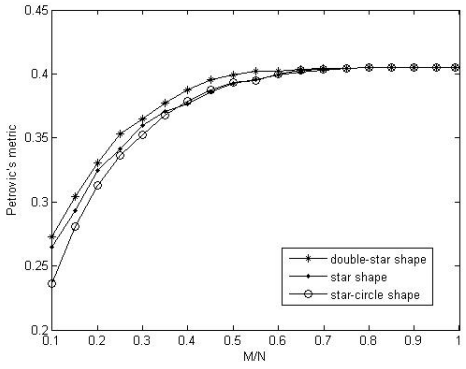

(b)

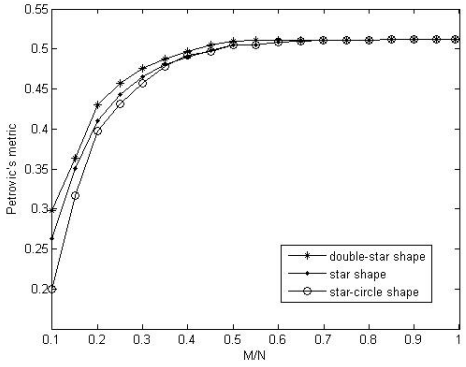

(c)

Figure 6: Petrovic's metric results using different sampling patterns for different images. (a) "Kayak" images. (b) "UN Camp" images. (c) Medical images.

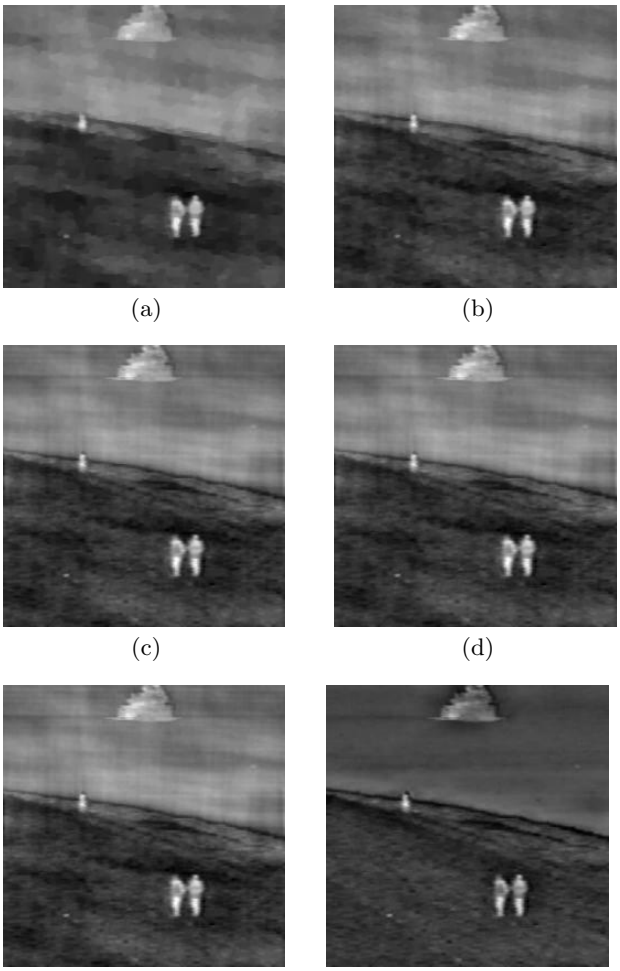

(a) (b) (c) (d) (e) (f)

Figure 7: Fusion results (The double-star-shaped sampling pattern is used here in the compressive image fusion algorithm). (a) Fused image recovered from $M = 6554$ compressive measurements ($M/N = 0.10$). (b) Fused image recovered from $M = 16384$ compressive measurements ($M/N = 0.25$). (c) Fused image recovered from $M = 32768$ compressive measurements ($M/N = 0.50$). (d) Fused image recovered from $M = 49152$ compressive measurements ($M/N = 0.75$). (e) Fused image using all Fourier coefficients ($N = 65536$). (f) Fused image using a MS scheme in the wavelet domain.

Compressive measurements are progressive in the sense that larger numbers of measurements will lead to higher quality reconstructed images. Image fusion can be performed without acquiring the observed signals. Additionally, the recently proposed compressive imaging system [10, 21], which relies on a single photon detector, enables imaging at new wavelengths unaccessible or prohibitively expensive using current focal plane imaging arrays. The development of this new imaging system has motivated investigation into CS-based image fusion techniques for practical use. This will significantly reduce the hardware cost, meanwhile expand image fusion in modern military and civilian imaging applications in a cheaper and more efficient way. However, the compressive measurements lose spatial information due to the CS measurement process. Therefore, traditional image fusion rules operating on local knowledge cannot be applied to compressive image fusion.

5. CONCLUSIONS AND FUTURE WORK

In this paper, we have presented a new image fusion algo-

rithm in the compressive domain, in which three sampling patterns were investigated for reconstruction from compressive samples. To the best of our knowledge, no literature has so far been focused on CS-based image fusion. One key advantage offered by this newly introduced technique is that samples can be collected without assuming any prior information about the signal being observed. Therefore, compressive image fusion provides a truly different way of fusing images compared with traditional fusion methods at pixel or feature level. Apart from computational and storage savings by using compressive sensing techniques, CS-based image fusion has a number of advantages over conventional image fusion algorithms. Most importantly, the recently developed compressive imaging system makes it promising to expand compressive image fusion in modern military and civilian imaging applications.

As we previously stated, the main weakness of compressive image fusion is that spatial information is lost due to compressive sensing measurement process. Consequently, conventional window-based fusion schemes cannot be applied to a CS-based fusion algorithm. By examining the underlying structure of the compressive measurements, a new fusion strategy could be derived in future work.

6. REFERENCES

[1] *The Online Resource for Research in Image Fusion*. avalable at http://www.imagefusion.org/.

[2] *The Berkeley Segmentation Dataset Benchmark*. University of California, Berkeley, CA, available at http://www.eecs.berkeley.edu/Research/Projects/CS-/vision/grouping/segbench/, Jul. 2003.

[3] M. Akcakaya and V. Tarokh. A frame construction and a universal distortion bound for sparse representations. *IEEE Tran. Sign. Process.*, 56(6):2443–2450, Jun. 2008.

[4] W. Bajwa, J. Haupt, A. Sayeed, and R. Nowak. Joint source-channel commnication for distributed estimation in sensor networks. *IEEE Trans. Inform. Theory*, 53(10):3629–3653, Oct. 2007.

[5] E. Candès and J. Romberg. *l1-magic: Recovery of sparse signal via convex programming*. code package available at http://www.l1-magic.org.

[6] E. Candès, J. Romberg, and T. Tao. Robust uncertainty principles: Exact signal reconstruction from highly incomplete frequency information. *IEEE Trans. Inform. Theory*, 56(2):489–509, 2006.

[7] E. Candès and T. Tao. Decoding by linear programming. *IEEE Trans. Inform. Theory*, 51(12):4203–4215, Dec. 2005.

[8] W. L. Chan, M. L. Moraverc, R. G. Baraniuk, and D. M. Mittleman. Terahertz imaging with compressed sensing and phase retrieval. *Optics Letters*, 33(9):974–976, May 2008.

[9] D. L. Donoho. Compressed sensing. *IEEE Trans. Inform. Theory*, 52(4):1289–1306, Apr. 2006.

[10] M. Duarte, M. Davenport, D. Takhar, J. Laska, T. Sun, K. Kelly, and R. Baraniuk. Single-pixel imaging via compressive sampling. *IEEE Signal Processing Magazine*, 25(2):83–91, Mar. 2008.

[11] K. Egiazarian, A. Foi, and V. Katkovnik. Compressed sensing image reconstruction via recursive spatially adaptive filtering. In *Proc. of the IEEE Int. Conf. Image Process.*, volume 1, pages 549–552, Sep. 2007.

[12] S. J. Kim, K. Koh, M. Lustig, and S. Boyd. An efficient method for compressed sensing. In *Proc. of the IEEE Int. Conf. Image Process.*, volume 3, pages 117–120, Sep. 2007.

[13] D. Marr. *Vision*. W. H. Freeman, New York, 1982.

[14] V. Petrovic and C. Xydeas. On the effects of sensor noise in pixel-level image fusion performance. In *Proc. of the Int. Conf. on Imag. Fus.*, volume 2, pages 14–19, Jul. 2000.

[15] G. Piella. A general framework for multiresolution image fusion: from pixels to regions. *Information Fusion*, 4:259–280, 2003.

[16] G. Piella and H. Heijmans. A new quality metric for image fusion. In *Proc. IEEE Conf. Image Process.*, volume 2, pages 173–176, 2003.

[17] J. Provost and F. Lesage. The application of compressed sensing for photo-acoustic tomography. *IEEE Trans. Med. imaging*, 28(4):585–594, Apr. 2009.

[18] G. Taubock and F. Hlawatsch. A compressed sensing technique for OFDM channel estimation in mobile environments: exploiting channel sparsity for reducting pilots. In *Proc. IEEE Conf. Acoustics, Speech and Signal Process.*, Mar. 2008.

[19] J. Trzasko and A. Manduca. Highly undersampled magnetic resonance image reconstruction via homotopic l_0-minimization. *IEEE Trans. Med. imaging*, 28(1):106–121, Jan. 2009.

[20] Y. Tsaig and D. L. Donoho. Extensions of compressed sensing. *Signal Process.*, 86:549–571, May. 2005.

[21] M. B. Wakin, J. N. Laska, M. F. Duarte, D. Baron, S. Sarvotham, D. Takhar, K. F. Kelly, and R. G. Baraniuk. An architecture for compressive imaging. In *Proc. of the IEEE Int. Conf. Image Process.*, pages 1273–1276, Oct. 2006.

[22] T. Wan, N. Canagarajah, and A. Achim. Region-based multisensor image fusion using generalized Gaussian distribution. In *Int. Workshop on Nonlinear Sign. and Image Process.*, Sep. 2007.

[23] T. Wan, N. Canagarajah, and A. Achim. Compressive image fusion. In *Proc. IEEE Int. Conf. Image Process.*, pages 1308–1311, 2008.

[24] T. Wan, N. Canagarajah, and A. Achim. Context enhancement through image fusion: A multiresolution approach based on convolution of cauchy distributions. In *Proc. IEEE Conf. Acoustics, Speech and Signal Process. (to appear)*, Mar. 2008.

[25] T. Wan, N. Canagarajah, and A. Achim. Segmentation-driven image fusion based on alpha-stable modeling of wavelet coefficients. *IEEE Trans. Multimedia*, 11(4):624–633, Jun. 2009.